COBEM 2023 27TH INTERNATIONAL CONGRESS OF MECHANICAL ENGENEERING
ABCM Brazilian Society of Mechanical Sciences and Engineering
27th ABCM International Congress of Mechanical Engineering
December 04-08, 2023, Florianópolis-SC, Brazil

COB-2023-1629
ELECTRIC VEHICLE BATTERY MODEL IDENTIFICATION FROM DATA COLLECTED IN DYNAMOMETER TEST CONDITIONS

Joaquim Manoel Gonçalves
Instituto Federal de Santa Catarina – Departament of Refrigeration and Climatization – São José – SC
joaquimm@ifsc.edu.br

Samuel Luna de Abreu
Instituto Federal de Santa Catarina – Departament of Refrigeration and Climatization – São José – SC
abreu@ifsc.edu.br

Murillo Stein
Universidade Federal de Santa Catarina – Department of Mechanical Engineering – Florianópolis – SC
murillo.stein8@gmail.com

Sergej Diel
Technische Hochschule Ingolstadt – Technische Mechanik und Numerische Methoden – Ingolstadt – Germany
sergej.diel@thi.de

Amir Antônio Martins de Oliveira Jr
Universidade Federal de Santa Catarina – Department of Mechanical Engineering – Florianópolis – SC
amir.oliveira@gmail.com

Rui Esteves Araújo
INESC TEC and Universidade do Porto – Faculdade de Engenharia – Department of Electrical Engineering – Porto – Portugal
raraujo@fe.up.pt

Abstract. *This study focused on developing a mathematical model for the State of Charge (SoC) of an electric vehicle battery. The research utilizes current, voltage, and temperature measurements obtained from a Nissan Leaf 2012 running on a chassis dynamometer at the Argonne National Laboratory (ANL). The SoC model is crucial in determining the available energy and range for the vehicle, and it plays a fundamental role in the design, simulation, and analysis of electric vehicle battery systems. The measurements were collected at a high sampling rate of 10Hz during a comprehensive two-and-a-half-hour test, which involved various drive schedules to ensure a complete battery discharge. The regenerative braking system in the vehicle generates charge and discharge currents that improved the quality of the data used in the development of the proposed methodology. It employed the least squares method to correlate the collected data and identify the model's parameters and coefficients. The developed SoC model consists of an equation that considers the battery voltage as a function of SoC, temperature, and current. It is divided into two parts: the pseudo-open circuit voltage (pseudo-OCV) curve and a complementary time series of currents with four different delay terms. Other variables such as power, energy, and internal resistance were analyzed. The identification of the battery's internal resistance allowed for the determination of heat losses and energy efficiency (98%). The errors in the developed model are uniformly distributed and the average of the absolute errors for the voltage curve is 0.25%, while considering the inverse solution process, the average of the absolute errors for the SoC is 2.5%.*

Keywords: *battery SoC model identification, li-ion batteries, electric vehicle batteries*

1. INTRODUCTION

The advent of electric vehicles brought the need for an accelerated development of electric battery technology to ensure better performance and cost reduction. There are several technologies used for the construction of battery cells, which can be separated into two groups: according to the chemistry used and according to the assembly geometry (Sterner and Stadler, 2019). Currently, the most used batteries for this application are Lithium Ion (Li-Ion) batteries, mainly due to their long lifespan, high energy density, low maintenance and no memory effect. On the other hand, the high cost and the possibility of damage and reduction of the useful life due to abusive use are problems to be solved (Diel et al., 2021). Abusive use must be understood not only associated with operating conditions outside the permitted limits, but also use in extreme conditions such as fast charging or high-power discharge due to the need to meet the demands of the vehicle dynamics in which the batteries are coupled. In addition, ambient temperature, both high and low, has additional implications for battery performance. Low temperatures require the battery to be preconditioned before use, and high temperatures accelerate aging and can damage the battery (Diel et al., 2021) and (Steger et al., 2022).

These situations described in the previous paragraph are common in electric vehicles, which causes the useful life to decrease significantly depending on the type of use given. Another particularity is that in the case of vehicles, the battery must be changed when it reaches 70-80% (Cherry, 2015) of its original electrical energy storage capacity. Because of this and to improve the performance of electric vehicles, several authors (Bernardi et al., 1985), (Doyle et al., 1993), (da Silva et al., 2021) and (Steger et al., 2022) have developed models to estimate the charge and discharge curves for later use, aiming to maintain the performance and extend the useful life as much as possible. It is important to highlight that good battery management throughout this first life in the car can even add value to the battery in its second life, where static applications can take advantage of the storage capacity still available (Kwade, 2020).

Models for estimating the operational parameters of batteries, in general, are developed from the voltage and current measured during their use, as proposed by Ahmed et al. (2020). Other authors seek greater accuracy with more complex models where other parameters are considered. In the present work, an electrothermal model that also considers temperature in addition to current and voltage is proposed. With the use of data measured in the battery combined with information obtained from dynamometer tests (Gonçalves at al., 2022), it was possible to identify the coefficients of the proposed model. An analysis of the obtained results indicates a good adherence between the model and experimental data. With the model, important driving information, such as temperature and State of Charge (SoC), can be simulated and a sensitivity analysis for selected parameters is also carried out.

State of Charge refers to the amount of energy remaining in a battery expressed as a percentage of its total electric charge nominal capacity. It represents the charge level of the battery at a specific point in time. The SoC is a critical parameter for monitoring and managing battery usage, as it provides information about the available energy and helps to prevent overcharging or deep discharging, which can be detrimental to the battery's performance and lifespan. In the context of an electric vehicle (EV) battery, monitoring the SoC is essential for determining the range and estimating the remaining driving distance vehicle autonomy. EVs typically display the SoC to inform drivers about the battery's charge level and help them plan their trips accordingly.

2. METHODOLOGY

The methodology section of this paper presents a comprehensive overview of the experimental procedures and analytical approaches employed to ensure the attainment of reliable results. To achieve this objective, several critical steps were undertaken. These steps form the foundation of our rigorous methodology, enabling the acquisition of robust and trustworthy results. In the subsequent sections, we will delve into each step in greater detail, elucidating the specific procedures and techniques employed throughout the research process.

To assess the State of Charge (SoC) of a battery, there are several methods and techniques that can be utilized. In a study conducted by Zhao et al. (2023), they provided an overview and explanation of commonly employed approaches, which can be summarized as follows:

a. Coulomb Counting: This method estimates the SOC by integrating the current flowing into or out of the battery over time. It requires accurate current measurements and may suffer from errors due to factors like self-discharge and voltage hysteresis.
b. Open Circuit Voltage (OCV): The OCV method utilizes the relationship between the battery's open circuit voltage and its SOC. By measuring the OCV and referencing it to a calibration curve or lookup table, the SOC can be estimated. Periodic calibration may be required to account for changes in internal resistance and other factors.
c. Model-Based Estimation: This approach employs mathematical models representing the battery's behavior and characteristics. It incorporates factors such as voltage, current, temperature, and nominal full capacity to estimate the SOC. Model-based approaches can provide accurate SOC estimations but may require initial calibration and ongoing parameter adjustments.
d. Kalman Filtering: Kalman filtering (Topan et al., 2016) is a state estimation technique that combines measurements and system dynamics to estimate the SOC. It utilizes current and voltage measurements, along with a battery model, to iteratively update and refine the SOC estimate. Kalman filters can offer robust SOC estimations but require a well-characterized battery model and accurate sensor measurements.

The model proposed in this study adopts a Model-Based Estimation approach. The comprehensive methodology for this process is presented in Figure (1) as a flowchart, illustrating the sequential steps involved. The following section describes each step in detail.

a. Data Collection: Perform dynamometer tests on the electric vehicle to collect relevant data. This may include measurements of voltage, current, temperature, and other parameters at various operating points and driving cycles. The tests should cover a wide range of operating conditions to capture the battery's behavior comprehensively.
b. Preprocessing: Clean and preprocess the collected data to remove noise, outliers, and inconsistencies. This step ensures that the data is accurate and reliable for further analysis.

c. Feature Extraction: Extract relevant features from the preprocessed data that are indicative of the battery's behavior. This may involve calculating parameters such as state of charge (SoC), internal resistance, power output, and efficiency.
d. Model Selection: Choose an appropriate model structure to represent the battery's behavior. Commonly used models include equivalent circuit models (e.g., Thevenin or internal resistance models) and physics-based models (e.g., electrochemical models).
e. Parameter Estimation: Estimate the model parameters based on the preprocessed data. This step involves finding the values for the model parameters that best fit the observed data. Optimization techniques such as least squares regression or maximum likelihood estimation are typically used for parameter estimation.
f. Model Refinement: If necessary, refine the model by iteratively repeating steps d to e. This may involve adjusting the model structure or fine-tuning the parameter estimation process to improve the model's accuracy.
g. Model Utilization: Once the battery model is identified and validated, it can be used for various purposes, such as battery management system development, energy management strategies, or system-level simulations.

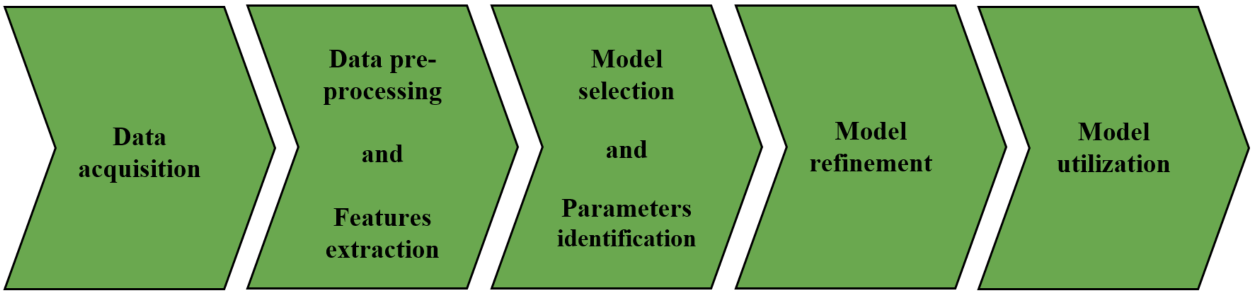

Figure 1. Schematic diagram of the proposed methodology.

2.1 Database

The dataset used for the development of the identification process is sourced from The Argonne National Laboratory (ANL, 2014) consists of data available in the Downloadable Dynamometer Database (D3), generated at the Advanced Powertrain Research Facility (APRF). This comprehensive database encompasses 10 different car models and includes the following variables: elapsed test time (s), speed (mph), force (N) at the contact point between the chassis dynamometer and vehicle wheels, battery pack electric current (A) and voltage (V), as well as temperature (Gonçalves et al., 2022).

For the purposes of the present study, data from a 2012 Nissan Leaf SV were utilized to develop and validate the model identification. The test duration spanned almost two and a half hours, during which various drive schedules were applied while maintaining a constant ambient temperature. Throughout the test, it was ensured that the battery was fully charged at the beginning, indicating a SoC of 100%. Likewise, at the end of the test, the battery was completely discharged, resulting in a SoC of 0%.

The vehicle was equipped with regenerative braking systems (Bravo et al., 2023) and (Lv et al., 2015), which enhanced the datasets by providing both positive and negative values of electric current, enabling more accurate determination of current effects by the internal resistances determined in the identification process (Lohse-Busch et al., 2012).

The measurements during the test were initially recorded at a sampling rate of 10 Hz. However, after data preprocessing, it was determined that a reduced sampling rate of 1 Hz was sufficient to maintain data integrity and accuracy. Battery state of charge (SoC) values were initially calculated using current measurements recorded at a sampling rate of 10 Hz. Subsequently, the data was filtered down to a sampling rate of 1 Hz. Upon re-calculating the SoC values using the filtered data in 1Hz, no significant differences were observed. This indicates that compressing the dataset, from 90,000 readings for each variable to 9,000 readings as it was in this case, is feasible and saves processing time facilitating a faster process.

2.2 Mathematical Model

In this section of the article, the equations and variables of the mathematical model used to numerically adjust its parameters are presented and described.

The electric charge refers to the amount, bookkeeping or inventory of electrons stored in the battery with a certain electrochemical electric field potential, as follows:

$$C(t) = C_0 - \int_0^t I(t) \cdot dt \qquad (1)$$

In Eq. (1), t is the time in hours, and $C(t)$ is the battery's electric charge in ampere-hours (1 Ah=2.247×10^{22} elementary charges). The equation is formulated as an analytical integral of the electric current $I(t)$, which is also a function of time. The parameter C_0 represents the initial battery charge at $t = 0$ and must be determined and known before conducting the test. The negative sign preceding the integral indicates that positive current values correspond to discharge currents, which occur when the vehicle is in driving mode. Conversely, negative current values are associated with regenerative energy systems, specifically when the vehicle is in braking mode.

$$C_i = C_{i-1} - (I_i + I_{i-1}) \cdot (t_i - t_{i-1})/2 \tag{2}$$

Equation (2) presents a computational format for numerically implementing the analytical integral expression from Eq. (1). The subscript (i) in this equation indicates the data point number being processed within the experimental dataset. To begin the integration process, it is necessary to set C_1 equal to the known battery initial charge ($C_1 = C_0$). From there, the integration starts at i=2 and continues until $i = N$, where N represents the total number of data points to be processed.

State of Charge refers to the amount of electric charge stored (remaining) in a battery expressed as a percentage of its nominal total electric charge capacity, as follows:

$$S_i = 100 \cdot C_i/C_t \qquad \text{or} \qquad S(t) = 100 \cdot C(t)/C_t \tag{3}$$

In Eq. (3), S is the percentual State of Charge (SoC) and C_t is the nominal "total" electric charge capacity of the battery. The term "nominal total electric charge capacity" refers to the maximum amount of electric charge that a battery is designed to hold under normal operating conditions. It represents the theoretical upper limit of the battery's storage capacity. This parameter also must be determined and known before conducting the test.

$$U_{p\_OCV} = k_0 + \frac{k_1}{s} + \frac{k_2}{s^2} + \frac{k_3}{s^3} + \frac{k_4}{s^4} + k_5 \cdot s + k_6 \cdot ln(s) + k_7 \cdot ln(1-s) + k_t \cdot (T - T_r) \tag{4}$$

$$s = (S/100) \cdot (1 - 2\varepsilon) + \varepsilon \tag{5}$$

Equation (4) represents the proposed model, based on that presented by Ahmed et al. (2020), for the battery pseudo-Open Circuit Voltage (pseudo-OCV), denoted as U_{p_OCV}, as a function of the normalized state of charge (s) and the battery temperature (T). The eight coefficients k_i (for i, 0 to 7) and k_t are constant parameters adjusted within the model. This equation is used to establish the relationship between the battery voltage and the SoC, also considering the temperature effects. The reference temperature T_r is a reference temperature freely choose and set, and in this work, it was set to 20 °C, by instance. By including the battery temperature into the equation, a comprehensive relationship between the battery voltage, state of charge, and temperature is established.

In Eq. (4), a normalized SoC, or linearly scaled, is included through a linear transformation of the original SoC, as defined in Eq. (5), denoted as S in uppercase to s in lowercase. This transformation is necessary to map the original SoC from the interval $[0.0\% \leq S \leq 100.0\%]$ to the interval $[\varepsilon \leq s \leq (1.0 - \varepsilon)]$ in order to avoid indeterminations in the terms $ln(s)$ and $ln(1-s)$ that would occur if values of 0.0 were reached in the logarithm function.

It is important to note that Eq. (4) does not account for the effect of electric current. It assumes the electric current to be zero, representing the battery in an open circuit. However, the voltage is function of the SoC and the temperature when the battery is in operation with a non-zero electric current, and in this way, the voltage calculated by this equation is referred to, and originally denominated in this work, as the Pseudo-Open Circuit Voltage of the battery.

$$U = U_{p\_OCV} + U_I \tag{6}$$

$$U_I = R_1 \cdot I_1 + R_2 \cdot I_2 + R_3 \cdot I_3 + R_4 \cdot I_4 \tag{7}$$

Equation (6) presents the comprehensive model proposed to describe the voltage curve of a battery during typical electric vehicle operation. This model incorporates both the electric current during discharging mode, which occurs during driving action, as well as during charging mode when the regenerative braking system is active. Thus, Equation (6) accounts for both positive electric currents associated with acceleration and negative electric currents associated with regenerative braking. It is composed of two terms: the first one is called pseudo-OCV, which has already been presented in Eq. (4); the second term (U_I) refers to the contributions of the electric current, modeled as a time series (Jeewandara et al, 2021), (Li et al, 2020) of 4 delay terms, as detailed in Eq. (7). The parameters R_j, where j varies from 1 to 4, represent the internal electrical resistances of the battery at the respective time delays t_j, and the same nomenclature logic is applied for the current terms (I_j) in the time series.

$$U = k_0 + \frac{k_1}{s} + \frac{k_2}{s^2} + \frac{k_3}{s^3} + \frac{k_4}{s^4} + k_5 \cdot s + k_6 \cdot ln(s) + k_7 \cdot ln(1-s) + k_t \cdot (T - T_r) + R_1 \cdot I_1 + R_2 \cdot I_2 + R_3 \cdot I_3 + R_4 \cdot I_4 \tag{8}$$

In Eq. (8), the complete expression for the voltage, $U=U(t)$, characteristic curve of the battery is presented as a function of the scaled state of charge $s=s(t)$, temperature $T(t)$, and electric current $I_j = I(t=t_j)$ in four time delays (j=1 to 4) terms.

2.3 Identification Process

The model identification process involves determining the parameters of the mathematical model presented in Eq. (8) using experimental data. This is achieved through the application of a regression data analysis using the least squares method, which allows for the estimation of the model parameters that best fit the experimental data.

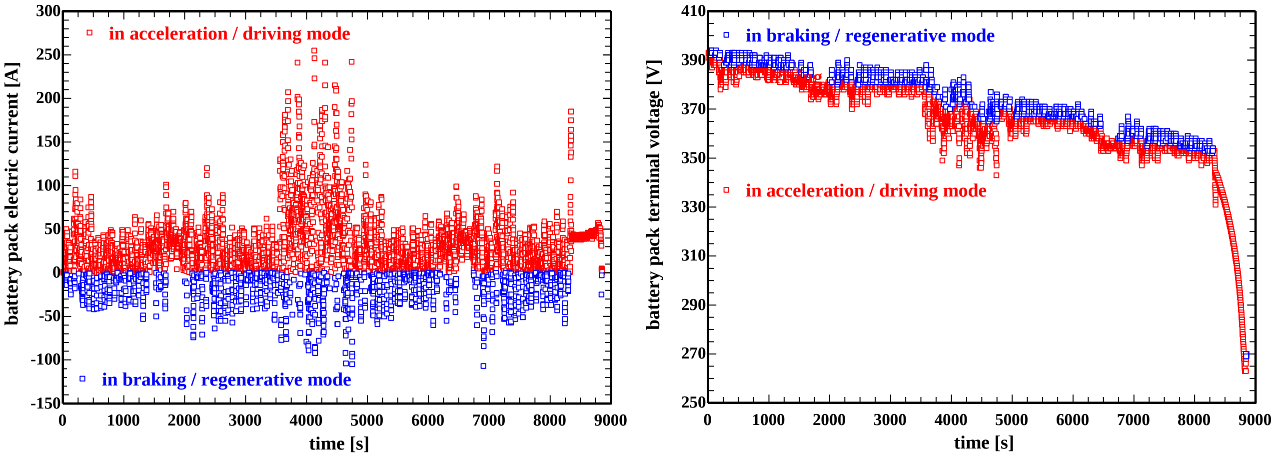

(a) Measured current versus time. (b) Measured voltage versus time.

Figure 2. Experimental current and voltage during the test.

Figure 2 graphically presents the experimental data of the two main variables used in the parameter identification process of the model. Figure 2(a) displays the electric current, while Figure 2(b) shows the battery terminals voltage during the test. The current values in Figure 2(a) range from around -50 A (blue points) to approximately +100 A (red points), with a period, after the first hour of testing, reaching peak values of around +200 A. Negative currents, the blue points, represent the operation of the regenerative braking system of the vehicle and reach values of approximately -50 A. In Figure 2(b), the typical behavior of voltage variation in lithium-ion vehicle batteries is observed. The voltage exhibits a small decline for most of the time, with a pronounced and almost abrupt drop in the final time segment.

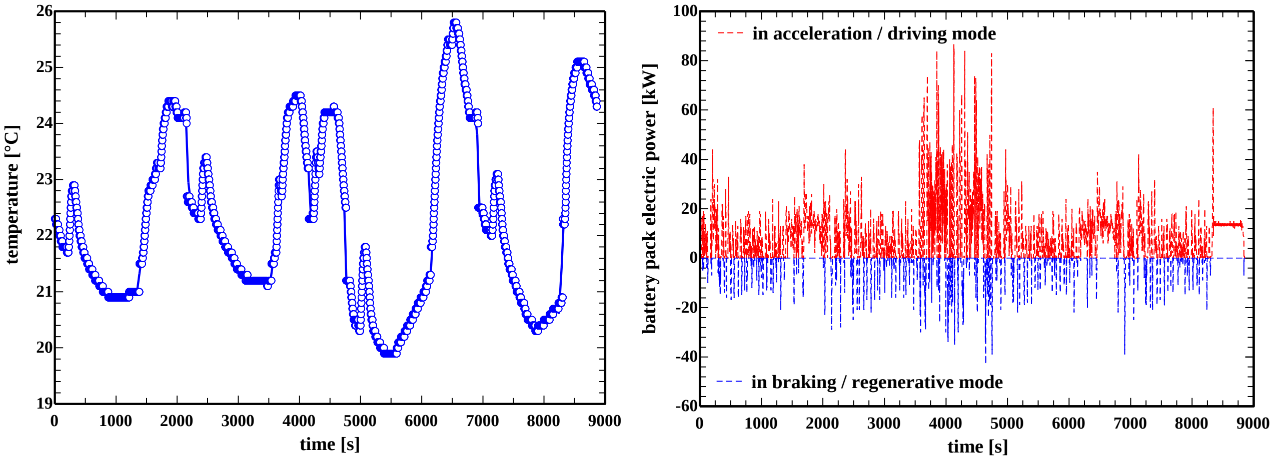

(a) Measured temperature versus time. (b) Calculated electric power versus time.

Figure 3. Experimental temperature and calculated power during the test.

Figure 3 presents the graphical representation of the measured temperature and the calculated battery electric power. The temperatures shown in Figure 3(a) exhibit various oscillations ranging from minimum values around 20°C to maximum values around 26°C. These oscillations result from variations in the demand for electric current or power from the different drive schedules to which the vehicle was subjected. The electric power, displayed in Figure 3(b), given in kW, is calculated by the product of voltage and current. Its values also vary and can be positive (red dashed line) or negative (blue dashed line), representing both acceleration and energy regeneration by the braking system.

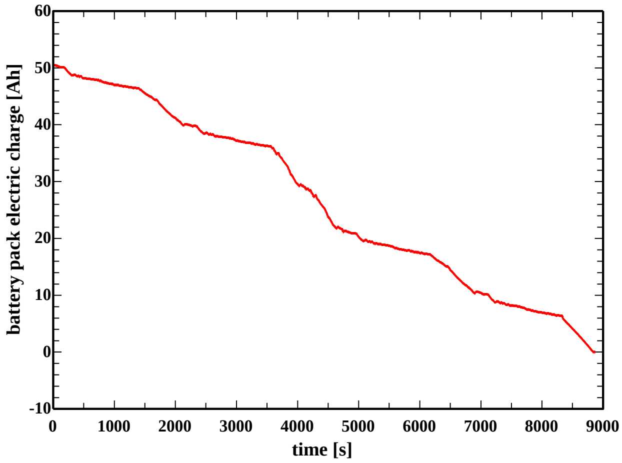

(a) Variation of battery electric charge during the test.

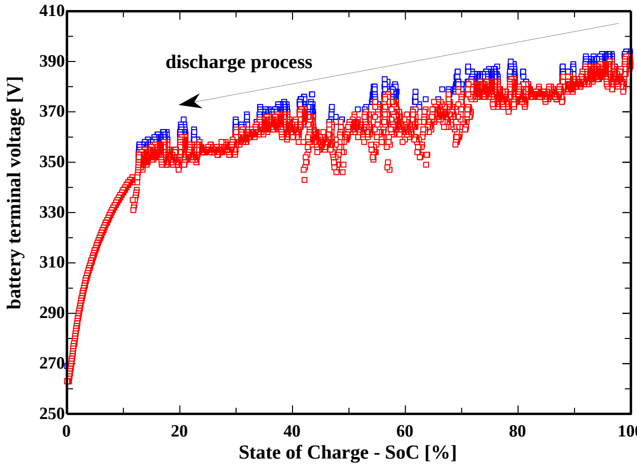

(b) Experimental voltage versus SoC.

Figure 4. Charge variation and voltage during the discharge test.

In Figure 4, the curves depicting the variation of electric charge and voltage as a function of State of Charge (SoC) are presented. To determine the electric charge capacity discharged, the numerical integration Eq. (2) was employed to current evolution during the test. Through this preprocessing, the total electric charge capacity discharge for the test was found to be 51.5 Ah. This value was then assumed and assigned to the initial charge (C_0) and total charge (C_t) parameters in Equations (1), (2), and (3). Thus, in Figure 4(a), the initial electric charge value at time zero is 51.5 Ah, and the electric charge value becomes zero at the end of the test. In Figure 4(b), the initial SoC value is 100%, and the final value is 0%. It is worth noting that the discharge process in Figure 4(b) occurs from right to left on the graph's scale, indicating a transition from 100% to 0% SoC, as it is also indicated by the arrow drawn above the points in this graph.

3. RESULTS AND ANALYSIS

At this stage, the experimental data has undergone preprocessing and is now prepared for the final identification of the voltage curve based on SoC, temperature, and electric current using the least squares method with Eq. (8) of the mathematical model. The preprocessing steps involved filtering the data from a 10 Hz sampling rate to 1Hz, calculating the total charge ($C_t = 51.5$ Ah) and initial charge ($C_0 = 51.5$ Ah), and removing data points with low voltage during the vehicle's startup and shutdown when transitioning between different drive schedules in the test.

Finally, before applying the least squares method, two additional parameters need to be set. The first parameter is epsilon ($\varepsilon = 0.05$) in Eq. (5). This scaling ensures that the SoC values are within a defined range $[0.05 \leq s \leq 0.95]$, excluding the extreme limits. The second parameter is the reference temperature ($T_r = 20$°C), which is directly incorporated into Eq. (8) of the model that will be adjusted during the identification process.

Table 1 provides the summary of the adjusted constants (k_i) and (k_t). Table 2 provides the summary of the internal resistance (R_j) values, with j=1 to 4, as described for Eq.(8), are for the four different delay terms: t_1=0, $t2$=10, $t3$=30, and $t4$=70 seconds, respectively, and all other 4 needed parameters that constitute the model proposed in this research.

Table 1. Summary of the model´s 8 constants (k_{i}), and k_t, identified by the least squares method.

k_0 [V]	k_1 [/]	k_2 [/]	k_3 [/]	k_4 [/]	k_5 [/]	k_6 [/]	k_7 [/]	k_t [V/K]
394.4	48.89	-4.769	0.2158	-0.003718	-54.59	109.3	-3.141	-0.7428

It is worthing to notice that the electric resistances in the time series, shown in Table 2, have reasonable values diminishing from just above 100 mOhm to just less than 5 mOhm as the time delay increases, from 0 to 70 s, in the series, being consistent with the physical phenomena of charge diffusion it represents in battery operation with transient currents. In fact, the consistency of these electric resistance values played a crucial role in guiding the trial and error process for determining the appropriate total number of terms and their times delays imposed on the time series during the iterative application of the least squares method until a successful correlation was achieved.

Table 2. Summary of the 4 terms of electric resistances (R_j) in the time series and all other 4 parameters needed.

R_1 [Ω]	R_2 [Ω]	R_3 [Ω]	R_4 [Ω]	C_0 [Ah]	C_t [Ah]	ε [/]	T_r [°C]
-0.1032	-0.01501	-0.009697	-0.004652	51.5	51.5	0.05	20

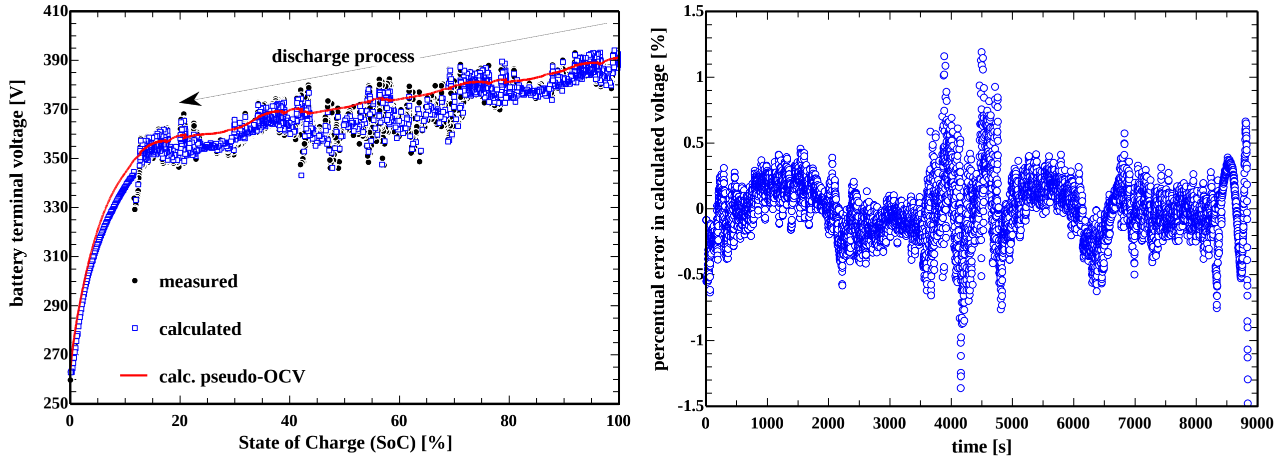

(a) Comparison of experimental and adjusted values.

(b) Errors (%) in the voltage (adjusted – measurements).

Figure 5. The identification process validation and errors.

A comparison between experimental and adjusted values, along with the resulting errors, is presented in Figure 5. Figure 5(a) shows the comparison of values, including the pseudo-OCV curve represented in red. The errors of the developed model are displayed in Figure 5(b). The errors exhibit a uniform distribution, indicating a consistent pattern, with an average absolute error of 0.25% for the voltage curve.

With the adjusted voltage equation identified, it was possible to analyze two important aspects of battery operation: 1) Determining State of Charge (SoC) from Voltage Readings: the equation was used to determine the SoC for different voltage readings. The relationship between voltage and SoC allows for monitoring the battery's energy level and estimating its remaining capacity. The results of this analysis are presented in Figure (6), and 2) Heat Dissipation due to Joule Heating: the battery's thermal resistances were identified, enabling the analysis of heat dissipation caused by Joule heating. This information is crucial for understanding and managing the battery's thermal behavior. The findings related to heat dissipation are presented in Figure (7).

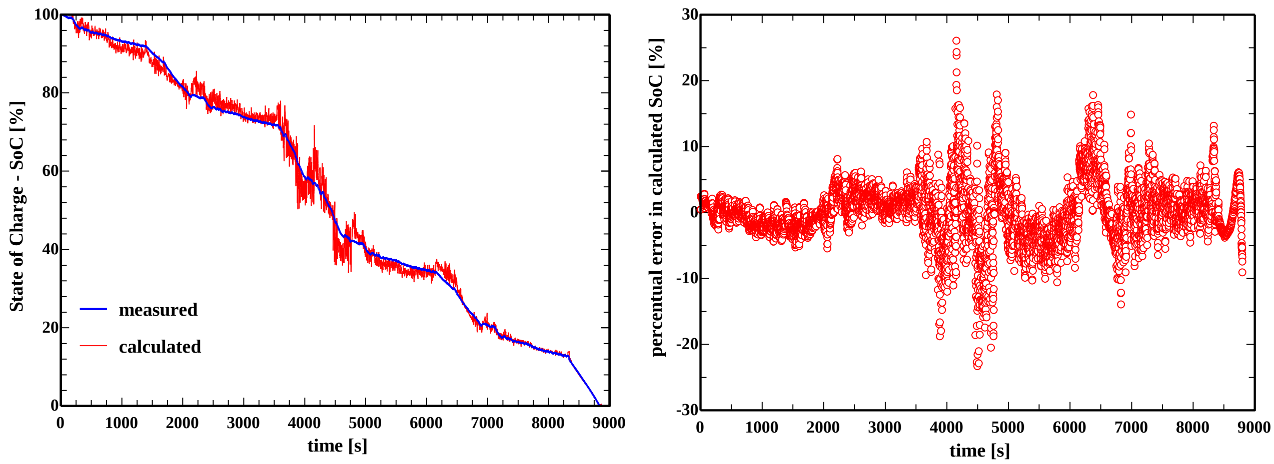

(a) SoC measured and calculated versus time.

(b) Errors in the inverse solution of Equation (8).

Figure 6. State of Charge (SoC) determined from voltage readings and its errors.

In Figure 6, a comparison between measured and experimental percentage State of Charge (SoC) is presented over the course of the test. The calculated values shown in Figure 6(a) are the result of the inverse solution obtained by applying the Newton-Raphson method to determine the SoC using Equation (8). This equation is non-linear and, in this inverse process, relies on input values of temperature, current, and voltage. The errors of the developed model, when used in this inverse way, are displayed in Figure 5(b). The errors exhibit a uniform distribution, indicating a consistent pattern, with an average absolute error of SoC equal to 2.5%.

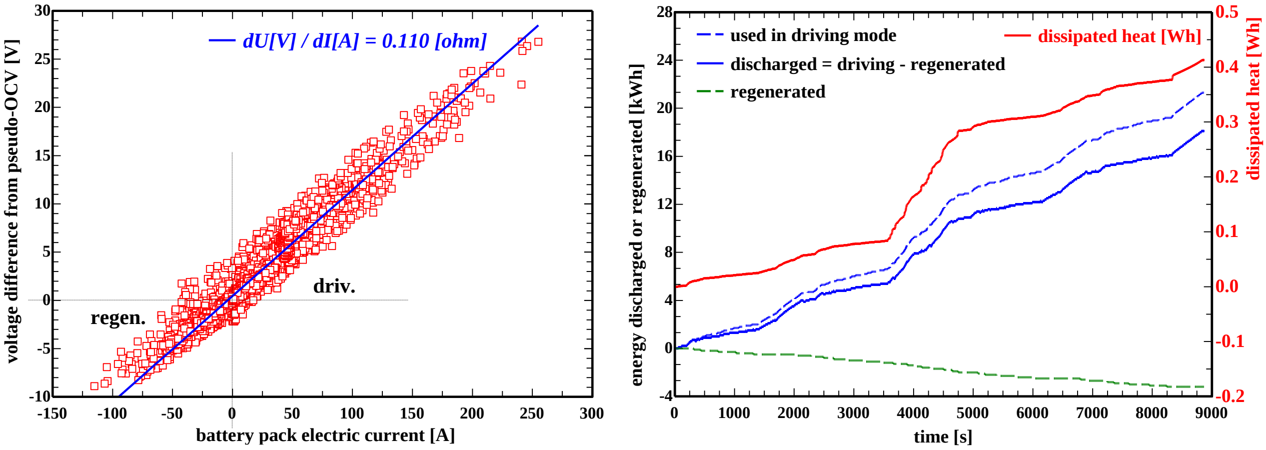

(a) Correlation between current and voltage.

(b) Energy discharged and heat losses in the battery.

Figure 7. Internal resistance identification graph and heat losses produced in the battery.

Figure 7(a) illustrates a correlation between current and voltage. The voltage displayed in this graph represents the difference between the measured voltage and the pseudo-OCV. This correlation demonstrates the influence of an internal electrical resistance, which encompasses the overpotential and underpotential voltages relative to the OCV curve during battery charging and discharging processes. By examining the slope of the line passing through the origin in this graph, the value of the internal electrical resistance of the battery can be determined, resulting in a value of 0.110 Ohm. It is worth of notice the notable consistency between the value of R_1 =103.5 mOhm obtained from the adjusted time series for the voltage curve presented in Equation (8) and Table 2, and the value of 110 mOhm derived from the graphical correlation depicted in Figure 7(a).

In Figure 7(b), the electric energy used for driving the vehicle during the test was 21.3 kWh. The regenerated fraction amounted to (-)3.2 kWh, and the difference between these values represented the energy actually discharged by the battery pack, which equaled 18.1 kWh. These energy values were depicted on the left scale of the graph in kWh. The thermal energy dissipated, or heat, due to the Joule effect caused by internal resistance, was 0.41 kWh and is shown by the red curve on the right scale of the graph in Wh. To calculate these energy amounts, the power was numerically integrated over time, similar to the approach used for electric charge in Eq. (2). The energies were determined from the electric power initially shown in Figure 3(b), while the dissipated heat was evaluated by multiplying the internal resistance by the square of the electric current. The energy recovered by the regenerative braking system accounted for 15% of the driving energy, and the heat loss in this case amounted to 2%, resulting in an overall energy efficiency of 98% for battery operation.

4. CONCLUSIONS AND FINAL REMARKS

In conclusion, this study presented a comprehensive methodology for developing a mathematical model to estimate the State of Charge (SoC) of electric vehicle batteries. The SoC curves derived from voltage measurements of a Nissan Leaf 2012 battery were obtained through a comprehensive test at the Argonne National Laboratory. The model identification process involved preprocessing the data, applying the least squares method to correlate the collected data, and determining the model's parameters and coefficients.

The developed SoC model incorporates an equation that considers battery voltage as a function of SoC, temperature, and current. It consists of a pseudo-open circuit voltage curve and a complementary time series of currents with four different delay terms: 0, 10, 30, and 70 seconds, respectively. The study demonstrated the accuracy and applicability of the inverse solution method used for the non-linear SoC equation. The developed model exhibited a uniform distribution of errors, with an average absolute error of 0.25% for the voltage curve and 2.5% for the SoC estimation.

Furthermore, the analysis of power, energy, and internal resistance allowed for the determination of heat losses and energy efficiency. It was found that the battery pack has an internal resistance of 110 mOhm, which causes a dissipation of 2% of the net energy balance of the battery as heat losses, resulting an overall energy efficiency of 98% for the battery operation and for the regenerative braking system a fraction of 15% of energy recovery was found.

This work contributes to the understanding and enhancement of electric vehicle battery systems, facilitating the design and optimization of energy management strategies. The developed model can be utilized to support the analysis, design, and control of battery thermal management systems for electric vehicles.

As a future step, it is proposed to apply the presented method using electric current profiles obtained from real-world driving conditions in battery cells or in a complete battery pack bench tests to get the data needed to characterize the SoC, thermal behavior, and aging of batteries in realistic situations.

5. ACKNOWLEDGEMENTS

We thank the GIZ-DAAD for funding this work through the 2LIFEBAT project number 57680517 approved on the program German-Brazilian research cooperation in the energy sector – NoPa 2.0.

6. REFERENCES

Ahmed, M. S., Raihan S. A., Balasingam, B., 2020. “A scaling approach for improved state of charge representation in rechargeable batteries”. Applied Energy 267 (2020) 114880. https://doi.org/10.1016/j.apenergy.2020.114880.

ANL, 2014. “Energy Systems D3 2012 Nissan Leaf SV”. Argonne National Laboratory, accessed in 10 Jun. 2023, https://www.anl.gov/taps/d3-2012-nissan-leaf.

Bernardi, D., Pawlikowski, E. and Newman, J., 1985. “A General Energy Balance for Battery Systems”. J. Electrochem. Soc., Vol. 132, No. 1, pp. 5-12.

Bravo, R. R. S., Gama, A. T. C., Oliveira, A. A. M., De Negri, V. J., 2023, “Component sizing and sensitivity analysis of design parameters of a hydraulic-pneumatic regenerative braking system for heavy duty vehicles”. Energy 264 (2023) 126021, https://doi.org/10.1016/j.energy.2022.126021.

Cherry, J., 2015. “Battery Durability in Electrified Vehicle Applications: A Review of Degradation Mechanisms and Durability Testing, Prepared by EPA, Final Report EP-C-12-014 WA 3-01 August 7, 2015.

Diel, S., Dörnhöfer, A., Müller, C., Bathe, M., 2021. “Strategies for Durability Validation of Traction Batteries and Fuel Cells”, DVM-Workshop in Fuel Cell, Battery, Electric Drive – Requirements and Validation, Ulm, 2021.

Doyle, M., Fuller, T. and Newman, J., 1993. “Modeling of Galvanostatic Charge and Discharge of the Lithium/Polymer/Insertion Cell”. J. Electrochem. Soc., Vol. 140, No. 6, pp. 1526-1533.

Gonçalves, J. M., de Abreu, S. L., dos Santos, L. A., Bresolin, A. A., Fuerback, A. L., Costa, D. G. , 2022. “Electrothermal Simulation of Electric Vehicle Battery under Driving Conditions”. 19th Brazilian Congress ENCIT-2022, https://www.sistema.abcm.org.br/articleFiles/download/36995 , Nov. 06th-10th, 2022, Bento Gonçalves, RS, Brazil.

Kwade, A., 2020. “Resource-Efficient Battery Life Cycles Driving Electric Mobility with the Circular Economy”. Circular Economy Initiative Deutschland (Eds.), Munich/London 2020. DOI: https://doi.org/10.48669/ceid_2021-2.

Jeewandara, J. M. D. S.; Karunadasa, J. P.; Hemapala, K. T. M. U, 2021. “SOC Level Estimation of Lithium-ion Battery Based on Time Series Forecasting Algorithms for Battery Management System”. In: 2021 3rd International Conference on Electrical Engineering (EECon). IEEE, 2021. p. 43-49.

Li, J.; Liu, M.; Jiang, Y., 2020. “SOC Estimation Based on Time Series Neural Network and Its Performance Evaluation”. In: Journal of Physics: Conference Series. IOP Publishing, 2020. p. 032072.

Lohse-Busch, H., Duoba, M., Rask, E., Meyer, M., 2012, "AVTA Nissan Leaf testing and analysis". Advanced Powertrain Research Facility, Argonne National Laboratory, 12 October 2012.

Lv, C.; Zhang, J., Li, Y., Yuan, Y., 2015. ”Mechanism analysis and evaluation methodology of regenerative braking contribution to energy efficiency improvement of electrified vehicles”. Energy C. and M., Vol. 92, pp. 469–482.

da Silva, C.T.; Dias, B.M.d.A.; Araujo, R.E.; Pellini, E.L.; Laganá, A.A.M., 2021. “Battery Model Identification Approach for Electric Forklift Application”. Energies 2021, 14, 6221. https://doi.org/10.3390/en14196221.

Steger, F.; Krogh, J.; Meegahapola, L.; Schweiger, H.-G., 2022. “Calculating Available Charge and Energy of Lithium-Ion Cells Based on OCV and Internal Resistance”. Energies 2022, 15, 7902. https:// doi.org/10.3390/en15217902.

Sterner, M., Stadler, I., 2019. “Handbook of Energy Storage: Demand, Technologies, Integration”. Translation of the 2nd German edition; Springer-Verlag.

Topan, P.A., Ramadan, M.N., Fathoni, G., Cahyadi, A.I. and Wahyunggoro, O., 2016, State of Charge (SOC) and State of Health (SOH) estimation on polymer lithium-polymer battery via Kalman filter, In Proceedings of the 2nd International Conference on Science and Technology-Computer (ICST), Yogyakarta, Indonesia, pp. 93-96.

Zhao, J.; Zhu, Y.; Zhang, B.; Liu, M.;Wang, J.; Liu, C.; Hao, X. , 2023, Review of State Estimation and Remaining Useful Life Prediction Methods for Lithium–Ion Batteries. Sustainability, 15, 5014. https://doi.org/10.3390/su15065014.

7. RESPONSIBILITY NOTICE

The authors are the only ones responsible for the printed material included in this paper.